

^7Li NMR study of the ordering phenomena in the intrinsic two-component magnetoelectric material $\text{Li}_2\text{ZrCuO}_4$

A. S. Moskvina,¹ E. Vavilova,^{2,3} S.-L. Drechsler,³ V. Kataev,³ and B. Büchner^{3,4}¹*Department of Theoretical Physics, Institute of Natural Sciences, Ural Federal University, 620083 Ekaterinburg, Russia*²*Zavoisky Physical-Technical Institute, Kazan Scientific Center of Russian Academy of Sciences, 420029 Kazan, Russia*³*Leibniz Institute for Solid State and Materials Research IFW Dresden, D-01171 Dresden, Germany*⁴*Institut für Festkörperphysik, Technische Universität Dresden, D-01062 Dresden, Germany*

(Received 23 September 2012; revised manuscript received 25 December 2012; published 5 February 2013)

We report an experimental and theoretical study of the low temperature ^7Li nuclear magnetic resonance (NMR) spectra of oriented powder samples of $\gamma\text{-Li}_2\text{ZrCuO}_4$ ($\equiv\text{Li}_2\text{CuZrO}_4$) which comprises interpenetrating sublattices of frustrated quasi-one-dimensional $s = 1/2$ quantum Heisenberg magnetic Cu^{2+} chains and frustrated quantum Ising electric sublattice of Li_I ions. Incommensurate spin order occurring in this compound at $T_N \simeq 6$ K gives rise to a drastic change of the ^7Li NMR spectrum. We show that the peculiar NMR line shapes are determined by the specific, sample dependent, distribution of the Li_I ions in the glassy ordered electric sublattice. The analysis of the NMR data in the framework of a spin-spiral model gives evidence for a remarkable interaction between magnetic and electric degrees of freedom in $\gamma\text{-Li}_2\text{ZrCuO}_4$, which suggests it as a promising model compound for fundamental studies of complex magnetoelectric phenomena and illustrates well their richness.

DOI: 10.1103/PhysRevB.87.054405

PACS number(s): 75.10.Pq, 76.60.-k, 77.80.-e

The coexistence and interplay of magnetic and electric degrees of freedom in the same material, called multiferroism, has been a subject of intense research worldwide in the last decade. One of the interesting aspects is the occurrence of incommensurate (spiral) spin structures in some of these materials, which give rise to peculiar magnetoelectric (ME) effects in the magnetically ordered phase (for a recent review see, e.g., Ref. 1). In this respect, the quantum spin-1/2 chain cuprate $\gamma\text{-Li}_2\text{ZrCuO}_4$ was reported recently to provide an interesting essentially new type of *intrinsic* two-component ME composites² where the quantum magnetism of CuO_2 chains meets the quantum (anti)ferro- or paraelectricity of an electrically active sublattice of tunneling Li^+ ions,³ which is spatially separated but still interacts with the magnetic subsystem. In the spin subsystem of this material frustrated quantum $s = 1/2$ J_1 - J_2 spin chains are realized in the CuO_2 chains of edge-shared CuO_4 plaquettes propagating along the c axis (see Ref. 4 and Fig. 1). Owing to residual three-dimensional (3D) interactions, magnetic order takes place at $T_N \simeq 6$ K, whereas the low temperature magnetic thermodynamics is strongly affected by a close proximity to the ferromagnetic quantum critical point (see Refs. 5 and 6). As predicted there on the basis of the calculated electronic and spin structures and fitted magnetic susceptibility and specific heat data (ignoring the weak interchain coupling),^{5,7} for the derived exchange integrals of the nearest (J_1) and the next-nearest (J_2) couplings between the Cu spins in the chain, a spin spiral structure should be realized in this system. Indeed, indications of the cycloidal ac plane spin spiral structure for CuO_2 chains in $\text{Li}_2\text{ZrCuO}_4$ with the theoretically proposed pitch angle of $\sim 33^\circ$ ⁵ have been found in recent ^7Li NMR experiments by Tarui *et al.*⁸

A unique feature of $\text{Li}_2\text{ZrCuO}_4$ is the presence of another, electrical degree of freedom. It is associated with the occurrence in the crystal structure, along with the regularly occupied Li_II site, of the split Li_I position,⁹ which is half-occupied (Fig. 1). We have argued in Ref. 3 that the charged Li^+

ion in the split position gives rise to a quantum Ising-like electric dipole oriented along the a axis. Experimentally, from measurements of ^7Li NMR and dielectric constants, it has been found that a 3D sublattice of these electrical pseudospins $\tau = 1/2$ orders glassylike at $T_g \sim 70$ K.³ Remarkably, as has been revealed by ESR spectroscopy, the electrical glass order yields a local Cu^{2+} ($S = 1/2$) site nonequivalence, suggestive of an interaction of interpenetrating electrical and magnetic sublattices.³

Here we show that the low-temperature ^7Li NMR measurements well below T_N provide an instructive tool to inspect peculiar features of both the magnetic and electric orderings in $\text{Li}_2\text{ZrCuO}_4$. The low-temperature ^7Li NMR measurements of oriented $\text{Li}_2\text{ZrCuO}_4$ polycrystalline samples were reported earlier in Ref. 8. However, two points justify a revision: (i) A glasslike structural ordering of the quantum paraelectric Li_I sublattice and hence, the $^7\text{Li}_\text{I}$ NMR line shape appears to be strongly affected by the sample history; and (ii) beyond the analysis given in Ref. 8, we now take into account specific features of the Li_I sublattice, revise, and advance the interpretation of the ^7Li NMR line shape. In particular, our results provide evidence for a remarkable interplay of the magnetic and electric sublattices in this new intrinsic two-component ME material. We note here that for usual multiferroics it is assumed the both magnetic and electric effects arise from a single center, i.e., they are one-component systems within our notation.

For the NMR measurements we have used the same a axis oriented powder samples of $\gamma\text{-Li}_2\text{ZrCuO}_4$ as in the previous work.³ The ^7Li ($I = 3/2$) NMR spectra were measured at low temperature both above and below T_N with a Tecmag pulse solid-state NMR spectrometer with a 9.2 T superconducting magnet from Magnex Scientific. The spectra were collected in two orientations of external magnetic field $\mathbf{H} \parallel \mathbf{a}$ and $\mathbf{H} \perp \mathbf{a}$ by a point-by-point acquisition of the Hahn echo intensity at a fixed frequency $\omega_N = 38$ MHz as a function of magnetic field. The shortest technically achievable separation

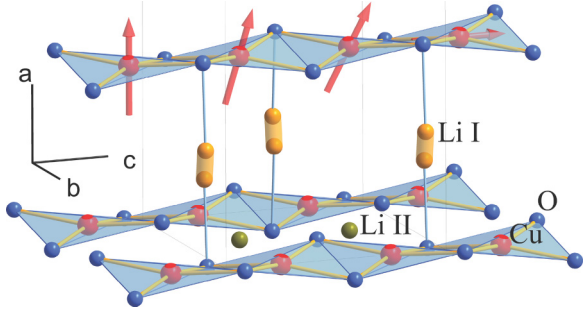


FIG. 1. (Color online) Interpenetrating spin-1/2 magnetic and pseudospin-1/2 electric sublattices in $\text{Li}_2\text{ZrCuO}_4$ associated with Cu^{2+} spins in the CuO_2 chains and with half-occupied Li_I split position, respectively. Arrows show schematically a possible spiral spin order in the CuO_2 chains.

time between the $\pi/2$ and π pulses $t = 8 \mu\text{s}$ was always used to minimize a possible influence of the transversal T_2 relaxation on the spectral shape. Indeed, we did not find across the measured spectrum substantial differences in the dependence of the echo intensity on t . The quadrupole splitting of the order of 0.05 MHz is typical for ^7Li nuclei in different cuprates^{10,11} and is unresolved in the Gaussian-like spectrum lines. Characteristic ^7Li NMR spectra are presented

in Figs. 2(a) and 2(b). At $\mathbf{H} \parallel \mathbf{a}$ partial contributions of $^7\text{Li}_\text{I}$ and $^7\text{Li}_\text{II}$ nuclei merge into a single Gaussian type line and we cannot distinguish these contributions above T_N . Yet, at $\mathbf{H} \perp \mathbf{a}$ we observe two well separated lines. Their high- T behavior was discussed in detail in Ref. 3, where an unambiguous assignment of the left and right lines to $^7\text{Li}_\text{I}$ (split position) and $^7\text{Li}_\text{II}$ nuclei (regular position), respectively, was made.¹² The present ^7Li NMR spectra measured at 10 K, i.e., above T_N , are very similar to those presented in Ref. 8.

A 3D magnetic ordering below T_N and the emergence of the internal fields from ordered Cu moments lead to dramatic changes in the ^7Li NMR spectra with a puzzling difference in line shapes for our samples and those studied in Ref. 8 (see Fig. 2). With the external field parallel to the a axis, we observe a broad main line with two symmetrically shifted shoulders, while in Ref. 8 one can see a well developed pedestal and the shoulders transformed into well separated satellites, Figs. 2(a) and 2(c), respectively. At $\mathbf{H} \perp \mathbf{a}$ we observe a broad asymmetric line with its center of gravity downshifted as compared with the paramagnetic case, while in Ref. 8 one can see a similar asymmetric downshifted line, however, with a well developed pedestal, Figs. 2(b) and 2(d), respectively.

The different line shapes and in particular the difference of the intensity of the wings between our spectra and those in

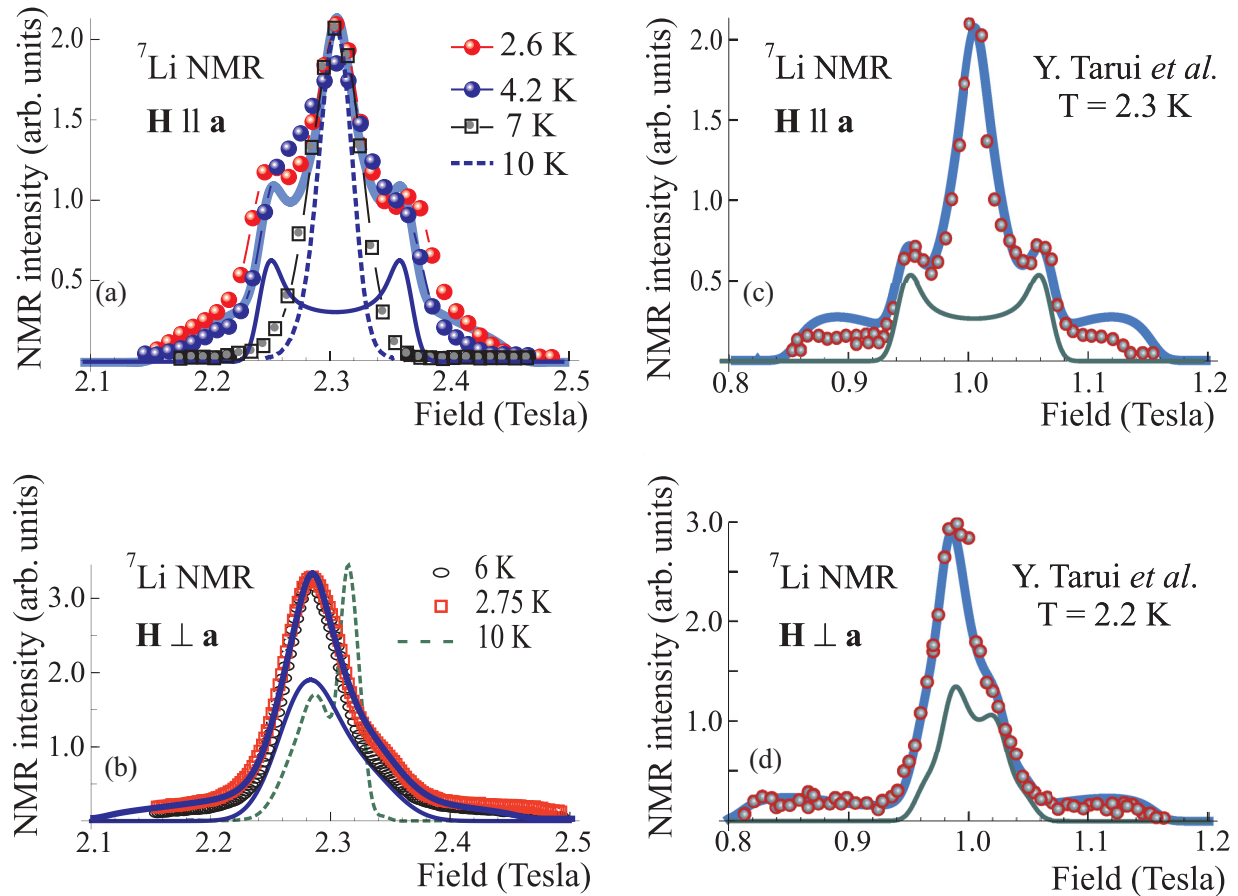


FIG. 2. (Color online) Comparison of low-temperature ^7Li NMR spectra of the $\text{Li}_2\text{ZrCuO}_4$ sample studied in the present work (left panel) and those from Ref. 8 (right panel). Thick solid lines: Results of the model fitting with different Li_I -distribution functions, f_1 (left panel) and f_3 (right panel), respectively (see the text). Thin solid lines: Partial contribution of the $^7\text{Li}_\text{II}$ NMR signal. Dashed lines in the left panel show the ^7Li NMR spectra at 10 K. (a) and (c) Low- T ^7Li NMR spectra obtained for $\mathbf{H} \parallel \mathbf{a}$. (b) and (d) Low- T ^7Li NMR spectra obtained for $\mathbf{H} \perp \mathbf{a}$.

Ref. 8 (Fig. 2) are unlikely to be attributed to the effect of the T_2 relaxation. The spectrum shown in Fig. 2(c) was measured in Ref. 8 with a much longer t value of $38 \mu\text{s}$ compared to the value of $8 \mu\text{s}$ which we used for the acquisition of the spectra in Fig. 2(a). If the difference in the wings were related to the T_2 effect, one would expect a smaller intensity at the wings in Fig. 2(c) compared to Fig. 2(a) due to a longer t in the former case. However, experimentally one finds the opposite behavior. The analysis of the ^7Li NMR line shapes in $\text{Li}_2\text{ZrCuO}_4$ and the elucidation of the above mentioned differences arising in the spectra at $T < T_N$ is the central point of the present work.

Despite extensive experimental and theoretical efforts during the last decades, the spin ordering in frustrated quasi-1D $s = 1/2$ quantum spin chains giving rise to spiral spin structures still remains a matter of broad activities, in particular regarding the use of the local nuclear probe techniques, such as nuclear quadrupole resonance and NMR.^{10,11,13} The hyperfine (HF) field induced by a classical planar spin helix on a nucleus positioned at a site \mathbf{R} near a CuO_2 chain is directly related to the local spin polarization on the adjacent sites $\mathbf{S}(\mathbf{R} + \mathbf{r})$: $\mathbf{h}(\mathbf{R}) = \sum_{\mathbf{r}} \hat{A}(\mathbf{r})\mathbf{S}(\mathbf{R} + \mathbf{r})$, where $\hat{A}(\mathbf{r})$ is the anisotropic HF tensor taking into account the magnetic dipole and the supertransferred Cu-O-Li HF interactions. The local field on both Li_I and Li_II nuclei is induced by a superposition of two adjacent spin spirals (see Fig. 1). Interestingly, irrespective of the relative phase shifts for the neighboring spirals, the HF field at an out-of-chain $^7\text{Li}_{\text{I,II}}$ nuclei can be written as follows:^{10,13}

$$h_{x,y,z} = A_{x,y,z}(q) \cos(qz + \alpha_{x,y,z}), \quad (1)$$

with the effective HF coupling parameters $A_{x,y,z}$ and the HF phase shifts $\alpha_{x,y,z}$, which generally may differ from the spin spiral phase shifts. Here \mathbf{q} is the propagation vector and z in the argument of cosine is a coordinate along the chain. A peculiar feature of the $^7\text{Li}_\text{I}$ nuclei is that their $A_{x,y,z}$ depend on the quantum mean value of the pseudospin z component $\langle \tau_z \rangle$ associated with the electrical dipole at the Li_I position as follows:

$$A_{x,y,z} = A_{x,y,z}^{(0)} + A_{x,y,z}^{(1)} \langle \tau_z \rangle. \quad (2)$$

Here $A^{(0)} = \frac{1}{2}[A^{(+)} + A^{(-)}]$, $A^{(1)} = [A^{(+)} - A^{(-)}]$, and $A^{(\pm)}$ are HF parameters for $^7\text{Li}_\text{I}$ nuclei at the up or down side of the split position, assigned to $\langle \tau_z \rangle = \pm \frac{1}{2}$, respectively. Equation (2) is a direct result of the quantum nature of the light Li_I ion in a two-well potential. The classical approach implies that the Li_I ion occupies only one of the wells at a time ($\langle \tau_z \rangle = \pm \frac{1}{2}$), while the quantum approach implies the realization of a superposition, or tunneling states with a certain probability to be localized in either well, hence, $-\frac{1}{2} \leq \langle \tau_z \rangle \leq +\frac{1}{2}$.

In a continuum approximation the $^7\text{Li}_\text{I}$ NMR line shape associated with a single nuclear $\Delta m_I = \pm 1$ transition can be calculated straightforwardly by a simple summation (integration):

$$F(\mathbf{H}) \propto \int_{-1}^{+1} f(\sigma) \int_0^{2\pi} \exp\{-[|\mathbf{H} + \mathbf{h}(\sigma, \phi)| - H_L]^2 / 2\delta^2\} \times d\sigma d\phi, \quad (3)$$

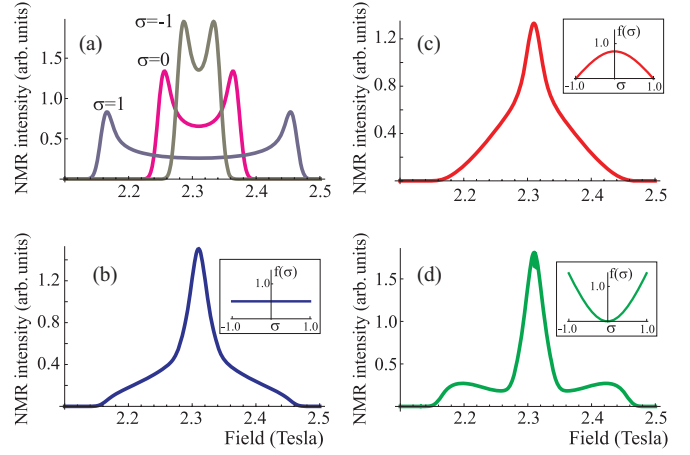


FIG. 3. (Color online) Simulation of the $^7\text{Li}_\text{I}$ NMR line shape with $A^{(0)} = 0.06 \text{ T}$, $A^{(1)} = 0.18 \text{ T}$, and different distribution of Li_I centers: (a) $\sigma = 0, \pm 1$; (b)–(d) $f(\sigma) = f_{1,2,3}(z)$, Eq. (4), respectively.

where $\sigma = 2\langle \tau_z \rangle$ ($-1 \leq \sigma \leq +1$), \mathbf{H} and H_L are the external and the resonance Larmor fields, respectively, $\phi = qz$, and δ denotes the homogeneous linewidth. In Eq. (3) a distribution function $f(\sigma)$ has been introduced.

Figure 3(a) shows the $^7\text{Li}_\text{I}$ NMR line shapes calculated for a specific structure of Li_I centers: $\sigma = \pm 1$ (classical positions) and $\sigma = 0$ (quantum superposition) with the HF parameters $A^{(0)} = 0.06 \text{ T}$, $A^{(1)} = 0.18 \text{ T}$, $H_L = 2.310 \text{ T}$, and the linewidth $\delta = 0.01 \text{ T}$.¹⁴ A two-peak hornlike line shape of the NMR signal is a typical signature of an infinite number of magnetically nonequivalent $^7\text{Li}_\text{I}$ sites characteristic of an incommensurate static modulation of the local magnetic fields (for details, see Refs. 10 and 13). However, in the case of a glassylike ordering of Li_I ions the function $f(\sigma)$ may have different forms depending on the character of the glass order which can be influenced, e.g., by the sample history and/or by subtle differences in the sample preparation. To be specific, below we address three types of the glasslike ordering with the following normalized distribution functions:

$$\begin{aligned} f_1(\sigma) &= \frac{1}{2}, & f_2(\sigma) &= \frac{\pi}{4} \cos \frac{\pi}{2} \sigma, \\ f_3(\sigma) &= \frac{\pi}{2\pi - 4} \left(1 - \cos \frac{\pi}{2} \sigma \right). \end{aligned} \quad (4)$$

They are plotted in the insets to Figs. 3(b)–3(d). The $f_1(\sigma)$ function describes a uniform σ distribution, while the $f_2(\sigma)$ and $f_3(\sigma)$ functions describe predominantly *quantum* and *classical* pseudospin orderings, respectively. Remarkably, taking into account the glasslike distribution of the mean Li_I positions [Eq. (4)] leads to dramatic changes of the $^7\text{Li}_\text{I}$ NMR line shape. Figures 3(b)–3(d) show the line shapes calculated with the same set of the single nucleus NMR parameters as in Fig. 3(a) but for the distributions characterized by the $f_{1,2,3}$ functions, respectively. Instead of a two-peak hornlike line shape, we arrive at a rather structureless single peak¹⁵ with a more or less pronounced pedestal. In particular, the pedestal distinctly displays a two-wing shape for the f_3 function, typical for a predominantly classical distribution of the Li_I positions. A drastic difference between the line shapes in Fig. 3(a) with those in Figs. 3(b)–3(d) clearly shows that the $^7\text{Li}_\text{I}$ NMR line

shape is strongly affected by the occurrence of the glasslike Li_I ordering and, moreover, is quite sensitive to the character of this order, which can be used for its detection and examination.

The apparent similarity of the NMR spectra modeled within the glass order scenarios with the experimental spectra at $T < T_N$ in Fig. 2 gives further strong support for the conclusion of our previous work³ on the glassy order of the electrical Li_I sublattice in $\text{Li}_2\text{ZrCuO}_4$. However, a closer comparison of those low-temperature ^7Li NMR spectra suggests essentially different glasslike Li_I distributions in the sample studied here [Figs. 2(a) and 2(b)] with that in Ref. 8 [Figs. 2(c) and 2(d)]. In particular, we can conclude that the Li_I distribution in our sample is close to that described by the f_1 function [Fig. 3(b)], suggesting an almost uniform distribution of different Li_I positions in the present case. On the contrary, the NMR line shape shown in Figs. 2(c) and 2(d) suggests that the Li_I distribution in the sample studied in Ref. 8 is close to that described by the function f_3 with an enhanced weight of extreme $\sigma = \pm 1$, or classical Li_I positions [Fig. 3(d)].

Furthermore, taking two essentially different distribution functions f_1 and f_3 [Eq. (4)] it is possible to model the NMR line shapes on a more quantitative level and to achieve a good agreement with the experimental spectra in the two respective cases (thick solid lines in Fig. 2). For that the overall contribution of the $^7\text{Li}_I$ nuclei to the NMR line shape was calculated assuming the same set of the HF parameters for both samples: $A_{\parallel}^{(0)} = 0.06$ T, $A_{\parallel}^{(1)} = 0.18$ T, $A_{\perp}^{(0)} = 0.071$ T, and $A_{\perp}^{(1)} = 0.106$ T. Here the subscripts \parallel and \perp denote the orientations $\mathbf{H} \parallel \mathbf{a}$ and $\mathbf{H} \perp \mathbf{a}$, respectively. Homogeneous isotropic linewidth $\delta = 0.01$ T was used in all cases. The following Larmor fields were taken for the modeling: $H_{L\parallel} = 2.310$ T and $H_{L\perp} = 2.283$ T for the spectra from the present work that corresponds to $H_{L\parallel} = 1.006$ T and $H_{L\perp} = 0.994$ T for spectra from Ref. 8.

The contribution of the immobile $^7\text{Li}_{II}$ nuclei at the regular positions to the total NMR signal at $\mathbf{H} \parallel \mathbf{a}$ was approximated for both samples by a two-peak hornlike curve. Since the signals from $^7\text{Li}_I$ and $^7\text{Li}_{II}$ nuclei overlap in the spectrum, we cannot discriminate between their T_2 contributions. Though we did not find a substantial difference in the dependence of the echo intensity on t across the spectrum, still some minor effects related to the shortest T_2 might be present. Therefore, the smaller spectral weight of the $^7\text{Li}_{II}$ line required for the modeling of the spectra [Fig. 2(b)] may be related to a shorter T_2 time (at the limit of the technically possible measurement conditions) of the $^7\text{Li}_{II}$ nuclei causing a partial wipeout of the $^7\text{Li}_{II}$ line. The best modeling was achieved with $A_{\parallel} = 0.06$ T and $\delta = 0.01$ T. The value of A_{\parallel} turns out to be the same as for the $^7\text{Li}_I$ nuclei, and the partial $^7\text{Li}_{II}$ -NMR signal corresponds therefore to the $\sigma = 0$ curve in Fig. 3(a). However, as will be seen below, the A parameters for $\mathbf{H} \perp \mathbf{a}$ are different for $^7\text{Li}_I$ and $^7\text{Li}_{II}$ nuclei. We mention once again that the simulated NMR spectra comprising the contributions from Li_I and Li_{II} sites in Figs. 2(a) and 2(c) are obtained with the same set of the HF parameters for both samples, however, with different distribution functions for Li_I , f_1 and f_3 , respectively.

The actual situation for the $\mathbf{H} \perp \mathbf{a}$ geometry in the a axis oriented polycrystals becomes more involved since we deal with the $^7\text{Li}_{II}$ NMR line shape formed by a superposition of at

least two contributions due to a random orientation of b and c axes. The two $^7\text{Li}_{II}$ contributions can be distinguished much clearer for the sample in Ref. 8 [thin solid line in Fig. 2(d)], where we assumed a superposition of two asymmetric hornlike curves,¹³ with $A_{\perp}^b = 0.022$ T and $A_{\perp}^c = 0.044$ T, respectively, and with the same Larmor field $H_L = 1.004$ T. The rather structureless line shape of the ^7Li NMR signal at $\mathbf{H} \perp \mathbf{a}$ for our sample does not allow a reliable separation of the two $^7\text{Li}_{II}$ NMR contributions. Thus, we restrain the model to a single broad asymmetric two-horn curve with $H_L = 2.310$ T, $A_{\perp}^{a,b} = 0.033$ T, and $\delta = 0.03$ T [thin solid line in Fig. 2(b)].

After all, despite still lacking knowledge on details of the incommensurate spin order in $\text{Li}_2\text{ZrCuO}_4$ yet to be elucidated, e.g., by neutron scattering, and a certain ambiguity in the estimates of the HF field,¹⁶ we have achieved a consistent description of the model given by Eq. (3), which is based on a spin-spiral scenario for the experimental ^7Li NMR line shapes of both samples under consideration (Fig. 2).¹⁷ Such a nice agreement not only supports the spin-spiral scenario for $\text{Li}_2\text{ZrCuO}_4$ proposed in Refs. 5 and 8, but also additionally justifies the occurrence of the electrical sublattice of Li_I^+ quantum dipoles, its glasslike ordering, and its interplay with the sublattice of quantum spin-1/2 chains.³ A 3D order of the incommensurate spin-1/2 sublattice makes visible a “fingerprint” of the glassylike ordered electrical sublattice in the ^7Li NMR spectra from which the particular character of the glass order can be deduced. The fact that these details turn out to be sample dependent is plausibly related to the sample history (e.g., differences in cooling/warming protocol in the NMR experiments) but also to subtle differences in the sample preparation (e.g., differences in concentrations of defects). It is worth noting that the glasslike Li_I ordering in $\text{Li}_2\text{ZrCuO}_4$ should give rise to strong fluctuations of the interchain exchange coupling in the CuO_2 chains via the local modulation of the Cu^{2+} crystal field (see the respective discussion in Ref. 3) and hence, to a sample dependent 3D magnetic ordering temperature T_N . Indeed, the $T_N \approx 6$ K for our sample is different from $T_N \approx 7$ K for the sample studied in Ref. 8.

In summary, we have studied both experimentally and theoretically the low-temperature ^7Li NMR line shapes in a axis oriented polycrystalline samples of $\gamma\text{-Li}_2\text{ZrCuO}_4$, which has been recently proposed as a new intrinsic magnetoelectric two-component material where a frustrated quasi-1D $s = 1/2$ quantum spin magnetic Cu^{2+} sublattice is interpenetrated by a frustrated 3D pseudospin-1/2 quantum Ising-glasslike electric Li_I^+ sublattice. We find that the onset of an incommensurate spin-spiral-like order below $T_N \approx 6$ K leads to a dramatic change of the ^7Li NMR spectrum whose line shape reflects the specific glasslike distribution of the Li_I ions and can be used for its examination. The proposed model of interacting incommensurate spin and glassy ordered electrical pseudospin sublattices enables a consistent description of the ^7Li NMR line shapes. We argue that a distinct difference of the ^7Li NMR spectra for the sample studied in the present work and the sample studied before in Ref. 8 emerging only below T_N is caused by different glasslike distributions of the Li_I ions with an almost uniform distribution of the mean Li_I positions in the former case and close to the classical one in the latter case. Such differences could be possibly ascribed to the sample history

or to differences in the sample preparation. Our experimental data and its theoretical analysis give therefore evidence for a remarkable interplay of the spin and pseudospin sublattices uniquely coexisting in $\text{Li}_2\text{ZrCuO}_4$ which put forward this compound as a promising model material for investigations of fundamental interactions between magnetic and electric degrees of freedom in complex transition metal oxides.

This work was supported by the German-Russian collaborative research grant of the Deutsche Forschungsgemeinschaft (DFG) BU 887/13-2 and of the Russian Foundation for Basic Research (RFBR) 12-02-91339-NNIO_a. A.S.M. acknowledges support of the RFBR (Grants No. 10-02-96032 and No. 12-02-01039). S.-L.D. acknowledges support by the DFG project DR269/3-1.

¹Y. Tokura and S. Seki, *Adv. Mat.* **22**, 1554 (2010).

² $\text{Li}_2\text{ZrCuO}_4$, to be considered here, is a ME composite on the atomic scale which is different from composite ME systems on a mesoscopic or nanoscale considered in the literature [see, e.g., S. Dussan *et al.*, *J. Phys.: Condens. Matter* **23**, 202203 (2011)].

³E. Vavilova *et al.*, *Europhys. Lett.* **88**, 27001 (2009).

⁴C. Dussarrat *et al.*, *J. Solid State Chem.* **166**, 311 (2002).

⁵S.-L. Drechsler *et al.*, *Phys. Rev. Lett.* **98**, 077202 (2007).

⁶M. Schmitt, J. Malek, S.-L. Drechsler, and H. Rosner, *Phys. Rev. B* **80**, 205111 (2009).

⁷J. Sirker, *Phys. Rev. B* **81**, 014419 (2010).

⁸Y. Tarui, Y. Kobayashi, and M. Sato, *J. Phys. Soc. Jpn.* **77**, 043703 (2008).

⁹At variance with Ref. 8 we hold the position labeling of original paper by Dussarat *et al.*⁴

¹⁰A. A. Gippius, E. N. Morozova, A. S. Moskvina, A. V. Zalesky, A. A. Bush, M. Baenitz, H. Rosner, and S.-L. Drechsler, *Phys. Rev. B* **70**, 020406 (2004).

¹¹C. Kegler, N. Buttgen, H. A. Krug von Nidda, A. Loidl, R. Nath, A. V. Mahajan, A. V. Prokofiev, and W. Amus, *Phys. Rev. B* **73**, 104418 (2006).

¹²We note that the different assignment of the left and the right lines in the ⁷Li NMR spectra at $\mathbf{H}_{\text{ext}} \perp \mathbf{a}$ to ⁷Li_{II} and ⁷Li_I nuclei, respectively, is not justified by our analysis given in Ref. 3.

¹³A. A. Gippius, A. S. Moskvina, and S.-L. Drechsler, *Phys. Rev. B* **77**, 180403 (2008).

¹⁴These particular parameter values are chosen to explain the ⁷Li_{II} contribution to the ⁷Li NMR signal later on in the text.

¹⁵The transformation of a two-peak spectrum in Fig. 3(a) into a single peak spectrum with shoulders [Figs. 3(b)–3(d)] is due to a σ -dependent contribution to the effective HF parameter A in Eq. (2). If $A(\sigma = 0)$ and $A(\sigma = \pm 1)$ have different signs, which can be achieved for a certain range of the values of $A^{(0)}$ and $A^{(1)}$, then $A(q)$ in Eq. (1) should inevitably be zero for certain q values giving rise to a peak in the integrated spectrum at the Larmor field H_L . In other words, with a continuous distribution of the Li_I positions given by Eq. (4) the peaks of the two-horn spectra in Fig. 3(a) will continuously move from the left to the right upon integration [Eq. (3)], overlapping in the center and making there a single peak.

¹⁶The detailed analysis of the microscopic HF tensor should take into account the hybridization effects between the lithium, oxygen, and copper sites which are obviously significant and determinant for the interplay between the electrical and spin sublattices.³ In our simplified model the effective HF parameters A in Eqs. (1) and (2) are merely fitting parameters that certainly cannot fully account for all details of the real material such as, e.g., an anisotropy of the spin spiral, a distortion of its shape by the Zeeman field, etc.

¹⁷The assumption of a substantial fraction of the so-called Li_{III} sites at the Cu positions made in Ref. 8 in order to explain the pedestal in the NMR line shape is unnecessary in our approach, where the pedestal naturally arises as a consequence of the f_3 -type distribution of the Li_I ions.